

## Author



June Tong joined a project at the Beckman Laser Institute that was using spatial frequency domain imaging to assess tissue health by calculating and generating images of tissue oxygen saturation. Her work involved developing a MATLAB algorithm to calculate color differences between digital images and, while she was primarily working as a programmer, she was able to observe closely the experimental process behind the research. June is particularly grateful to Dr. Adrien Ponticorvo, who played an integral role in mentoring her throughout the project. She hopes to continue her education by going on to medical school and studying to become a prosthetist.

### Key Terms

- ◆ CIELAB 1976
- ◆ Delta E
- ◆ Modulated Imaging
- ◆ Region of Interest
- ◆ RGB
- ◆ Tissue Flaps

# Quantifying Color Difference: A Comparison between Spatial Frequency Domain Imaging to Digital Color Imaging in Assessment of Reconstructive Flap Occlusions

**June Tong**  
*Biomedical Engineering*

## Abstract

Tissue transfer techniques using tissue flaps are commonly used in reconstructive surgery to replace damaged tissue. While typically successful, tissue flaps that require additional surgery have a 40–60% failure rate. The current technique to diagnose tissue flap failure is to monitor the flap hourly and look for signs of discoloration. The chance of salvaging a tissue flap improves the earlier a problem becomes apparent; therefore, a technique that can detect changes before they are visually noticeable has the potential to improve post-operative flap management. This project used spatial frequency domain imaging (SFDI) to generate images of tissue oxygen saturation and compare the results to imaged clinical appearance. To mimic different levels of tissue failure, flaps were created in a swine model in which blood flow was monitored with ultrasound probes and controlled with vascular occlusion cuffs. Blood flow was reduced by 25%, 50%, 75%, and 100% of baseline values. The color changes were recorded in digital camera images and quantified to predict which occlusion conditions would be visible to the human eye. The results were compared to the SFDI oxygen saturation images. Results indicate that while the human eye can reliably perceive changes at 100% occlusion, SFDI is able to detect changes as small as 25%, thereby improving response time and reducing the potential for flap failure.

## Faculty Mentor



Early identification of surgically reconstructed tissue in the post-operative period is critical to reducing complications. We are developing new quantitative optical imaging techniques that have potential to enable rapid identification of early changes that indicate flap dysfunction. In order to assess the performance of our new methods, we must also quantify current approaches to flap surveillance. The most commonly employed existing approach to flap surveillance is simple visual inspection. The work presented here quantifies the color changes associated with visual inspection (using digital photography as a record) in order to enable a performance comparison to the metrics associated with our new technology, which is based on near infrared light.

**Anthony J. Durkin**  
*School of Medicine*

## Introduction

### Transfer Tissue Flaps

A typical procedure in reconstructive surgery to repair damaged tissue from breast cancer and general trauma is to transfer donor tissue (intact with skin, adipose tissues, minor muscles and connective tissues) to the recipient site (Smith et al., 2010). Generally, these transferred tissues (known as tissue flaps) have a low failure rate (5–10%), but flaps requiring additional surgeries after complications have a 40–60% failure rate (Chen et al., 2007; Kroll et al., 1996; Steele, 2011). Complications primarily result from the faulty reattachment of the blood vasculature in the procedure, possibly resulting in occlusions in these arteries or veins (Chen et al., 2007). This is more common and lethal in the veins, as venous occlusions can pool deoxygenated blood into the capillaries and inhibit oxygen diffusion into the tissue. Arterial occlusions can also occur, but are not as common or lethal due to the arteries' higher blood pressure.

Failing flaps are often difficult to detect because of the lack of immediate visible complications; occlusions can develop gradually over time with slight observable signs in their early stages, yet few animal studies are dedicated to studying these partial occlusions (Russell et al., 2006). Most studies focus on the ability to detect complete occlusions, but occluded tissue flaps may have already become necrotic at that point, resulting in the partial or complete loss of the tissue mass. Detection of the early stages of occlusion is vital to improve the salvage rates of compromised flaps (Kroll et al., 1996; Bui et al., 2007).

### Methods of Studying Occlusions

In order to provide a more quantitative evaluation of vascular occlusions, several studies were conducted to investigate techniques to study tissue flaps. Laser Doppler Imaging has been used successfully in animals to detect partial occlusions (Gimbel et al., 2009), and Doppler ultrasound has been used to monitor tissue flaps post operatively in humans (Lorenzetti et al., 2002; Vakharia et al., 2012). Near-infrared spectroscopy has also proven to be useful in identifying occlusions in animals (Thorniley et al., 1998; Pharaon et al., 2010; Yafi et al., 2011; Matsui et al., 2009) and monitoring humans in a clinical setting (Steele, 2011; Whitaker et al., 2011). The main drawbacks to these techniques have been their lack of ability to identify small problematic areas of tissue and large time consumption. While all of these techniques have been used with varying levels of effectiveness to study tissue flaps, it is difficult to measure how much benefit they provide beyond what can be assessed by basic human monitoring.

The current standard for diagnosing occlusion in the tissues after surgery is periodic monitoring of characteristics such as temperature and, especially, discoloration (Bui et al., 2007; Russell et al., 2006; Chubb et al., 2012). Color changes in occluded tissue have been quantified before, typically with a colorimeter (Russell et al., 2006); however, recent studies have indicated that color differences in digital color images show similar results (Miyamoto et al., 2002; Leon et al., 2006). This is typically accomplished by normalizing the color images to a standard scale and evaluating color differences with respect to the scale.

### Color Spaces

Color can be quantified in digital images, which are generated in a red, green and blue (RGB) color space. The RGB color space is device dependent on the camera, in that the generated range of colors in the image is relative to its white point (the lightest color of the image). Consequently, the numerical RGB values assigned to each pixel of the image would be inconsistent if the environmental setup changed. Thus, RGB values are typically normalized to a standard scale (typically CIE 1976  $L^*a^*b^*$ ) in order to mimic the nonlinear response of the eye (Miyamoto et al., 2002; Leon et al., 2006).

CIE 1976  $L^*a^*b^*$  (CIELAB or LAB) is a uniform color scale specifically designed to map color perception accurately. The LAB color model uses lightness ( $L^*$ ), the red to green axis ( $a^*$ ), and the blue to yellow axis ( $b^*$ ), which are plotted at right angles to one another to form a three-dimensional coordinate system (Figure 1). The structure of the  $L^*a^*b^*$  color space is based on the theory that a color cannot be simultaneously green and red, nor blue and yellow. As a result, red/green and yellow/blue colors can be described with single numeric values respective to the axes.

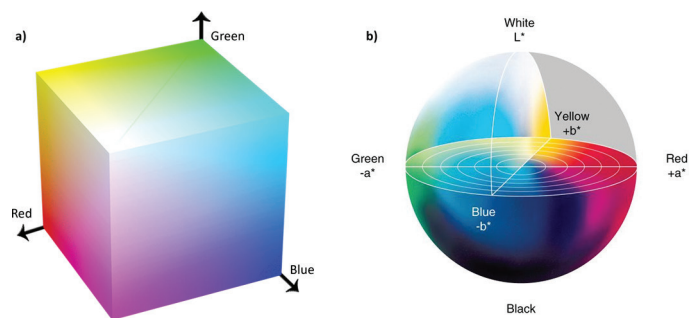


Figure 1

3D representations of (A) RGB and (B) CIELAB color space values. The RGB color space is a cube that can change its axes depending on the relative white point in the image, whereas the CIELAB color space is a sphere that has set axes.

By normalizing the scale to a uniform color space, the distance metric  $\Delta E_{ab}^*$  (delta E, dE, or  $\Delta E$ ) between two LAB values ( $L_1^*$ ,  $a_1^*$ ,  $b_1^*$ ) and ( $L_2^*$ ,  $a_2^*$ ,  $b_2^*$ ) can be used to quantify color differences (Equation 1).

$$\Delta E_{ab}^* = \sqrt{(L_1^* - L_2^*)^2 + (a_1^* - a_2^*)^2 + (b_1^* - b_2^*)^2} \quad (1)$$

It is possible to determine a  $\Delta E$  value at which human vision can determine color difference. This just noticeable difference (JND) for the human eye to detect color change has been recorded to be  $\Delta E$  values from 1 to 3 (Hill et al., 1997; Stokes et al., 1992; Ikeda et al., 1992; Mahy et al., 1991). Previous studies focusing on the JND of skin have indicated that a  $\Delta E$  below 3 represents an unnoticeable color change (Vander et al., 2000). In this study, the  $\Delta E$  of occlusions were quantified in comparison to oxygen saturation images generated by spatial frequency domain imaging.

### Spatial Frequency Domain Imaging

Spatial Frequency Domain Imaging (SFDI) is a novel non-invasive optical imaging technology that was developed at the Beckman Laser Institute. SFDI allows for wide-field quantitative mapping of tissue optical properties through its capability of spatially resolving optical absorption and scattering parameters (Cuccia et al., 2009). The system separates and quantifies the multi-spectral absorption and scattering optical properties, providing a more direct assessment of tissue via the derivation of physiologically relevant parameters (Cuccia et al., 2009). SFDI is able to use multiple wavelengths and spatial frequencies to generate chromophore maps of the oxygenated hemoglobin in the tissue.

SFDI uses spatially-modulated illumination to image tissue constituents, where periodic illumination patterns of various spatial frequencies project over a large area of a sample. The tissue is illuminated with a spatial pattern of the form:

$$S = \frac{S_0}{2} [1 + M_0 \cos(2\pi f_s x + \alpha)] \quad (2)$$

$S_0$ ,  $M_0$ ,  $f_s$ , and  $\alpha$  are the illumination source intensity, modulation depth, spatial frequency, and spatial phase, respectively.

Since oxygenated and deoxygenated hemoglobin return different absorption values, which correlate to respective measured concentrations, the total oxygen saturation in a tissue flap can be defined by measuring oxygenated hemoglobin concentration (HbO<sub>2</sub>), deoxygenated hemoglobin concentration (Hb), total hemoglobin concentration (HbO<sub>2</sub> + Hb), and oxygen saturation (stO<sub>2</sub>) (Equation 3). Normal

levels of oxygenated hemoglobin in tissue are known to be around 70–80%.

$$StO_2 = \frac{[HbO_2]}{[HbO_2] + [Hb]} \quad (3)$$

The key components of SFDI are outlined in Figure 2.

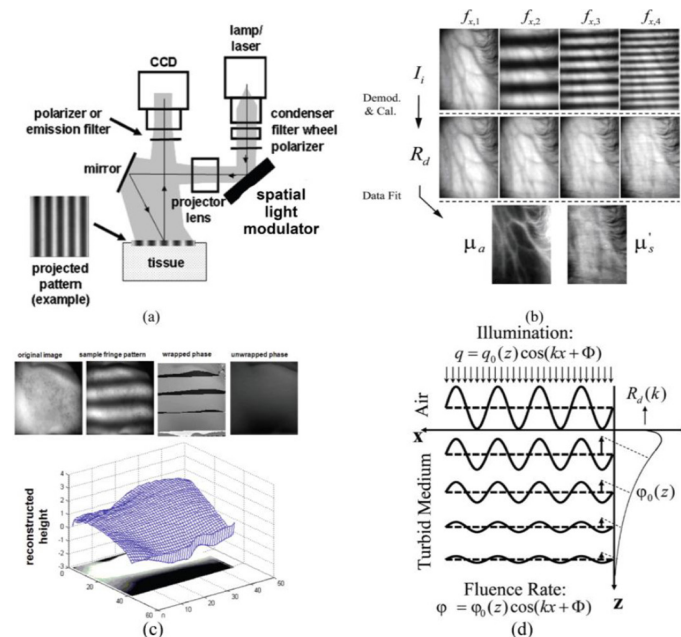


Figure 2

SFDI method summary. (A) SFDI platform. (B) Flowchart of data processing: Intensity data at each frequency (three phase images per frequency) are amplitude, demodulated, calibrated, and fit. Data are processed separately for each pixel, generating spatial maps of optical properties. (C) Phase data provide topology information which can be used for correction of curvature-related illumination non-uniformities. (D) Schematic of modulated illumination source and the resulting modulated internal fluency rate.

This imaging technique can quantify and generate images of tissue oxygen saturation. SFDI has the potential to be an ideal tool for studying tissue flaps because of its quick, non-invasive data acquisition. It has been used in previous studies to quantify changes in physiological parameters for complete and partial vascular occlusions, but was not assessed relative to human monitoring (Pharaon et al., 2010; Gioux et al., 2011; Ponticorvo et al., 2013).

### Case Study

Since vascular compromise can be nearly unnoticeable to the human eye, salvaging the tissue flaps necessitates earlier detection of occlusions in the tissue (Chen et al., 2007; Steele, 2011). In this study we determined the JND of different levels of partial occlusions in porcine tissue com-

pared to SFDI results to assay the benefits of the imaging technique for studying tissue flaps.

## Experimental Design

### Surgical Procedures

Experiments were performed under the University of California, Irvine Institutional Animal Care Use Committee protocol #2006-2693. Eight Yorkshire pigs were anesthetized with ketamine (20 mg/kg, xylazine (2 mg/kg) and pentobarbital (10 mg/kg). The pigs were mechanically ventilated with oxygen (100%) and isoflurane (1–1.5%), while body temperature (36–38 °C) was maintained with a heating pad. Two 12 x 7 cm bilateral inferior epigastric myocutaneous flaps were raised in the abdomen (Figure 3A). The deep inferior epigastric vasculature was isolated in the tissue in order to ensure that only one set of vessels would be connected to the flap. The surgical process was repeated on both flaps, with one of the flaps to serve as the control group during the experiment. Half of the animals were studied under arterial occlusion, while the other half of the animals were studied under venous occlusion. A New Era NE-1000 syringe pump injected saline into a Docsx Biomedical occlusion balloon cuff placed on either the artery or vein, which would inflate and restrict blood flow. The blood flow was monitored with a Transonic System TS-240 ultrasound probe attached to the artery or vein being occluded (Figure 3B). Approximately one hour after completing the surgery, baseline blood flow was recorded in both flaps. The average arterial blood flow in all the animals was 11.6 ml/min, and the average venous blood flow was

15.4 ml/min. To induce partial occlusions in the tissue flaps, the occlusion cuff was programmed to inflate and reduce baseline values by 25%, 50%, 75%, and 100% for 30 min each, punctuated with intermediary resting periods of 30 min. Typical blood flow time courses are shown in Figure 3 (C,D). The process typically took less than four min for the occlusion cuff to achieve the respective blood flow.

### Color Difference Calculations

RGB images of the tissues were taken from a digital camera, which had a field of view of 13.5 x 10.5 cm. A white LED projected light to capture an RGB image for color analysis, each sequence of data collection about 42 s apart. MATLAB (R2011b, Mathworks, Natick, MA) was used to convert RGB images from the digital camera to CIELAB images. Once each pixel of the image was represented in the LAB color space and a baseline image was established, a  $\Delta E$  value was created at each time point via Equation 1. To ensure that the  $\Delta E$  calculations were made in a homogeneous region across time, two regions of interest (ROI), approximately 2 x 2 cm, were drawn within the first baseline digital image. Every other image after that had the ROI in the same position. The  $\Delta E$  values within the ROIs were averaged in order to account for any external motion within the successive pictures after the baseline image. A diagram of the  $\Delta E$  calculations is summarized in Figure 4.

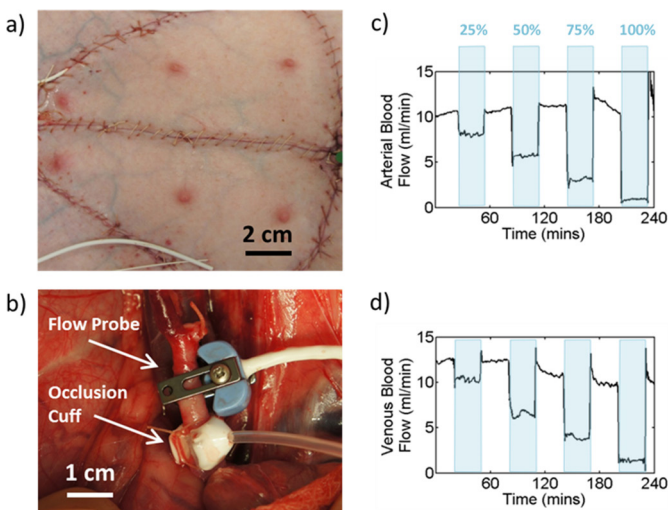


**Figure 3**  
Swine pedicle flap preparation from the: (A) top view and (B) under-side with labeled instrumentation. Typical time course of blood flow changes with labeled partial occlusion levels in the: (C) artery and (D) vein.

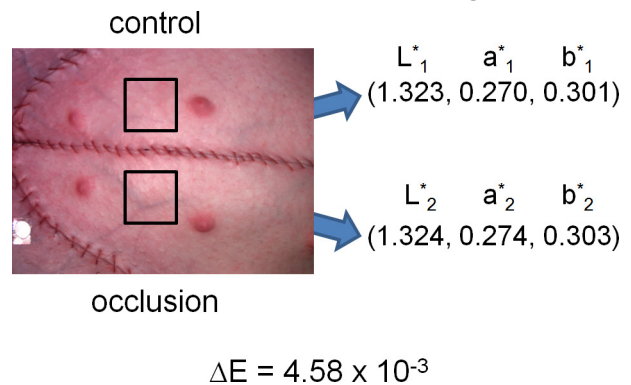


**Figure 4**  
An example of the color change calculations in the flaps. The average LAB color within the ROI allows for the calculation of  $\Delta E$  via the distance metric (Equation 1).

### SFDI System and Calculations

The setup for the imaging technique has been described in a previous study (Cuccia et al., 2009), but an overview is provided in Figure 5. A prototype clinic-compatible near-infrared camera v100 from Modulated Imaging Inc. was used to collect the flap data. The SFDI system employed light from LEDs of 658, 730, and 850 nm wavelength that was expanded onto a spatial light modulator (Digital Micromirror Device Discovery™ 1100, Texas Instruments, Dallas,

TX). The field of view of the near-infrared camera was 13.5 x 10.5 cm. A sinusoidal pattern of two frequencies (0 and 0.2 mm<sup>-1</sup>) was projected at three phases (0°, 12°, and 240°) by each of the LEDs. Each sequencing of data took approximately 12 s, and the process was repeated every 30 s. Custom C# software (Modulated Imaging Inc., Irvine, CA) was used to control the hardware. A diagram of the imaging technique is shown in Figure 5.

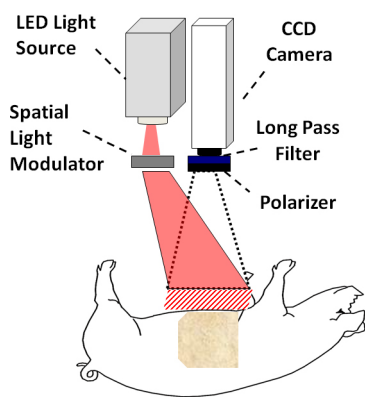


**Figure 5**  
General overview of the imaging and feedback occlusion systems.

Custom software was written in MATLAB for SFDI analysis of the collected images as described previously (Cuccia et al., 2009). These values were used to estimate the absorption and reduced scattering coefficient properties based on a scaled Monte Carlo generated lookup table at each wavelength (Erickson et al., 2010). After a surface profiling, a calibration measurement from a sample with known optical properties was used to correct for errors resulting from surface curvature (Gioux et al., 2009). The absorption maps were used to generate chromophore concentration maps of oxygenated and deoxygenated hemoglobin that could be converted to stO<sub>2</sub> chromophore maps via Equation 2.

## Results

Each of the following figures shows RGB images along with  $\Delta E$  and  $\Delta \text{stO}_2$  images overlaid at each respective time point during 25%, 50%, 75%, and 100% occlusion. The time points correspond to the baseline image taken before the occlusion and the midpoint of each occlusion level (approximately 15 min after the start of the occlusion). The  $\Delta E$  images threshold at the JND value of 3 to depict the visible color change. In order to avoid noise in the SFDI images, the  $\Delta \text{stO}_2$  images are also set to a threshold of 3%.

### Venous Occlusion

The venous occlusion experiment with the most significant color changes (Figure 6) at the 100% occlusion level also had noticeable color changes at the 75% level, but no noticeable changes at the smaller occlusion levels beyond the movement associated with a large vein. The  $\Delta \text{stO}_2$  changes, on the other hand, could be seen throughout the flap at the 100%, 75%, and 50% occlusion levels, with a few spatially sporadic changes at the 25% occlusion level.

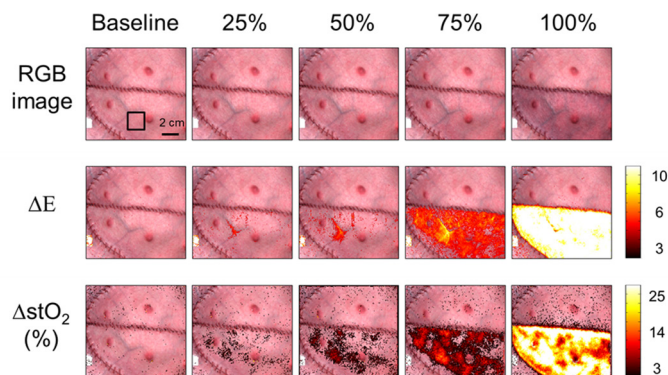


**Figure 6**  
Color images layered with  $\Delta E$  images and  $\Delta \text{stO}_2$  images at different time points corresponding to different occlusion levels from a venous experiment that showed the most significant color changes.

The venous occlusion experiment with the least significant color changes (Figure 7) at the 100% occlusion level only had perceivable changes at that level with a few scattered noticeable changes at the 75% level. Despite this, the  $\Delta \text{stO}_2$  could again be seen throughout the majority of the flap at the 100%, 75%, and 50% occlusion levels.

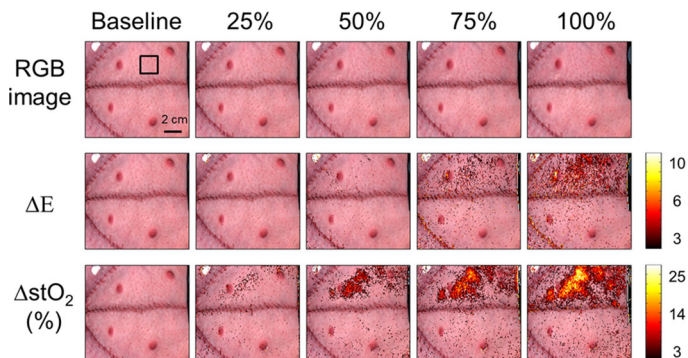


**Figure 7**  
Color images layered with  $\Delta E$  images and  $\Delta \text{stO}_2$  images at different time points corresponding to different occlusion levels from a venous experiment that showed the least significant color changes.

The time courses of both parameters in a given ROI for each partial venous occlusion experiment are shown in Figure 8. They verify that distinct stO<sub>2</sub> changes can be seen

at 50%, 75% and 100% across all experiments. They also highlight the variability of the  $\Delta E$  changes. There is a wide range of values for  $\Delta E$  at the 75% and 100% occlusion levels that vary from above 10 to barely at the JND of 3. Also, no changes in color were noticeable at the 25% or 50% occlusion level in any of the animals.

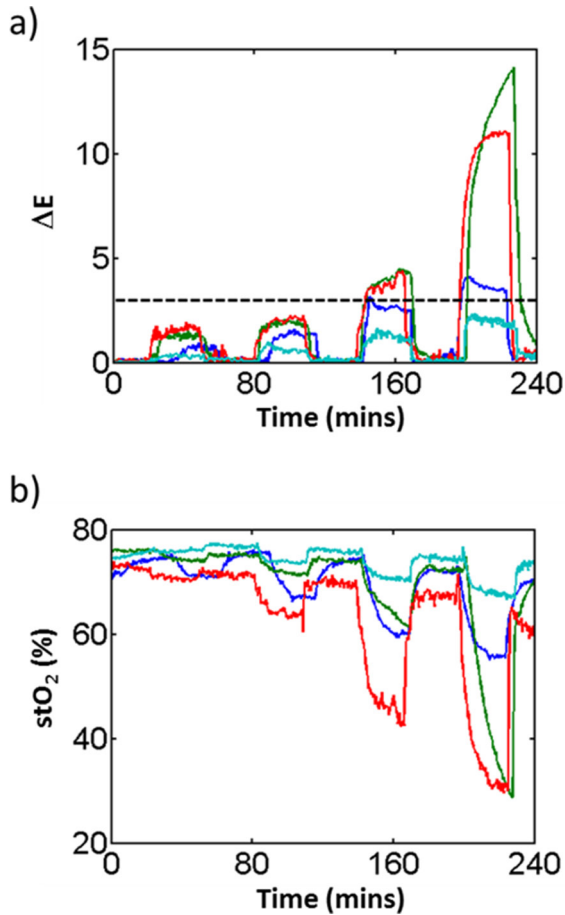


Figure 8  
The time courses of (A)  $\Delta E$  changes and (B)  $\Delta stO_2$  changes across all venous occlusion experiments.

### Arterial Occlusion

A montage of images from a typical arterial occlusion experiment is shown in Figure 9. There are noticeable changes throughout the flap at the 100% occlusion level and scattered noticeable changes at the 75% level. However, significant  $\Delta stO_2$  values are seen throughout the majority of the flap at all occlusion levels.

The time courses of  $\Delta E$  and  $\Delta stO_2$  for a given ROI in each partial arterial occlusion experiment are shown in Figure 10. They verify that distinct  $stO_2$  changes can be seen at 50%, 75% and 100% across all experiments and again highlight the variability of the  $\Delta E$  changes. There is a wide range of values for  $\Delta E$  at the 100% occlusion level that range from

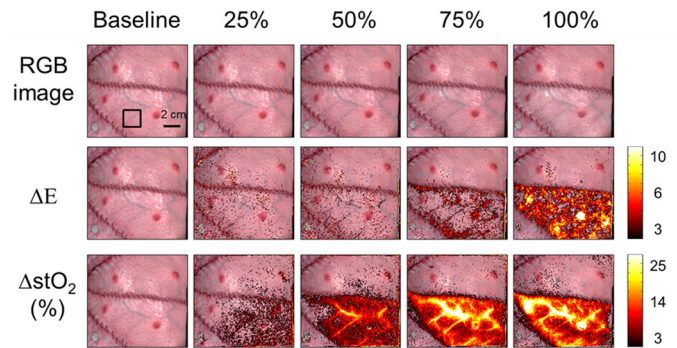


Figure 9  
Color images, overlaid  $\Delta E$  images, and overlaid  $\Delta stO_2$  images at different time points corresponding to different occlusion levels from a typical arterial occlusion experiment.

above 7 to barely above the JND of 3. At the 75% occlusion level the color changes were just below the JND, while no changes in color were noticeable at the 25% or 50% occlusion levels.

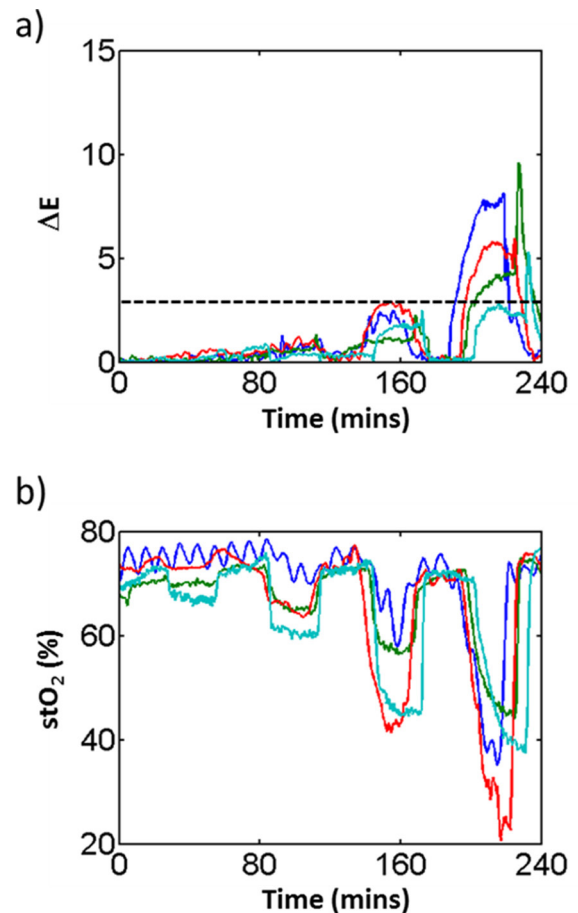


Figure 10  
The time courses of (A)  $\Delta E$  changes and (B)  $\Delta stO_2$  changes across all arterial occlusion experiments.

## Discussion

Both vascular occlusions demonstrated that for 50% occlusion and below, the human eye would not be able to detect color difference easily, whereas SFDI could detect occlusions as early as 25%. The findings suggest that SFDI can provide earlier detection of vascular insufficiency compared to the current standard of monitoring the patients. Although serial examination of the tissue flaps includes other variables such as temperature and texture, a previous study indicates that in spite of these factors, human observation of color change is the primary diagnostic technique (Chubb et al., 2012). As indicated by this and several other studies though, the color change in the flap can be a variable and sometimes false indicator of tissue health (Chubb et al., 2010; Pohlenz et al., 2007; Bui et al., 2007). Another factor of color change to indicate tissue health could be the time length of the occlusion; this study observed each occlusion level for only 30 min. A previous study observed its occlusion levels on an hourly basis, which indicated a detectable color change for occlusions as low as 30% under this time period (Chen et al., 2007). However, regardless of the period of assessment, the fact that SFDI can observe occlusions present for less than 30 min in the vasculature is a testament to the imaging technique's sensitivity.

Some errors that occurred during the experiment were the consequence of an increase in external light. A limitation of the device is the need for a dark room so that the projected light can be fully analyzed. One pig model exhibited failing physiological parameters during the imaging, which required the room lights to be turned on to observe and resuscitate the swine properly. The increase in light amplified the  $\Delta E$  and  $\Delta \text{stO}_2$  data; however, the results may not be entirely artificial, since the blood flow data also decreased severely during the occlusions. Another limitation for SFDI is that the analyzed light does not penetrate very deep into the skin (~1 cm), so occlusions deeper in the tissue may not be detected. However, the instrumentation would still be a useful tool because it is a quick, non-invasive method that quantifies tissue oxygen saturation.

## Conclusion

With the quantification of [HbO], [Hb], [HbT], and [StO<sub>2</sub>], SFDI has the potential to assist postoperative care via an objective and visual assessment of physiological parameters. The results of SFDI relative to visible color change suggest that the imaging instrumentation will provide a quantitative, accurate technique to assess vascular occlusions. Future potential uses of SFDI include imaging before, during

and after surgery to properly assess tissue flap conditions in patients. With further development to shrink the SFDI machinery to a portable point-of-care device, future works may reduce the number of compromised flaps that leave the operating room and decrease health care costs related to flap reconstruction.

## Acknowledgements

I would like to acknowledge Dr. Tony Durkin and Dr. Adrien Ponticorvo for their mentorship throughout the project, which would not have been possible without their immense efforts, patience, and guidance. I thank UROP and SURP for funding the project. Finally, I would like to thank NIH and the Beckman Laser Institute for their support, including P41EB015890 (A Biomedical Technology Resource) from NIBIB and R42GM077713 from NIGMS.

## Works Cited

- Bui, Duc T., Peter G. Cordeiro, Qun-Yikng Hu, Joseph J. Disa, Andrea Pusic, and Babak J. Mehrara. "Free flap reexploration: indications, treatment, and outcomes in 1193 free flaps." *Plastic and Reconstructive Surgery* 119.7 (2007): 2092-2100.
- Chen, Kuang-Te, Samir Mardini, David C. Chuang, Chih-Hung Lin, Ming-Huei Cheng, Yu-Te Lin, Wei-Chao Huang, Chung-Kan Tsao, and Fu-Chan Wei. "Timing of presentation of the first signs of vascular compromise dictates the salvage outcome of free flap transfers." *Plastic and Reconstructive Surgery* 120.1 (2007): 187-195.
- Cheon, Young W., Won J. Lee, and Dong K. Rah. "Objective and quantitative evaluation of scar color using the L\*a\*b\* color coordinates." *The Journal of Craniofacial Surgery* 21.3 (2010): 679-684.
- Chubb, Daniel, Iain S. Whitaker, Warren M. Rozen, and Mark W. Ashton. "Continued Observations in the Postoperative Monitoring of Free Flaps: Preliminary Experiences with Masimo Radical-7 Transcutaneous Plethysmography and Pulse Oximetry." *Plastic and Reconstructive Surgery* 129.1 (2012): 222e-223e.
- Chubb, Daniel, Warren M. Rozen, Iain S. Whitaker, Rafael Acosta, Damien Grinsell, and Mark W. Ashton. "The Efficacy of Clinical Assessment in the Postoperative Monitoring of Free Flaps: A Review of 1140 Consecutive Cases." *Plastic and Reconstructive Surgery* 125.4 (2010): 1157-1166.

- Cuccia, David J., Frederic Bevilacqua, Anthony J. Durkin, Frederick R. Ayers, and Bruce J. Tromberg. "Quantitation and Mapping of Tissue Optical Properties Using Modulated Imaging." *Journal of Biomedical Optics* 14.2 (2009): 024012.
- Erickson, Tim A., Amaan Mazhar, David J. Cuccia, Anthony J. Durkin, and James W. Tunnell. "Lookup-table method for imaging optical properties with structured illumination beyond the diffusion theory regime." *Journal of Biomedical Optics* 15.3 (2010): 036013.
- Gimbel, Michael L., Mark D. Rollins, Eri Fukaya, and Harriet W. Hopf. "Monitoring Partial and Full Venous Outflow Compromise in a Rabbit Skin Flap Model." *Plastic and Reconstructive Surgery* 124.3 (2009): 796–803.
- Gioux, Sylvain, Amaan Mazhar, Bernard T. Lee, Samuel J. Lin, Adam M. Tobia, David J. Cuccia, Alan Stockdale, Rafiou Oketokoun, Yoshitomo Ashitate, Edward Kelly, Maxwell Weinmann, Nicholas J. Durr, Lorissa A. Moffitt, Anthony J. Durkin, Bruce J. Tromberg, and John V. Frangioni. "First-in-human Pilot Study of a Spatial Frequency Domain Oxygenation Imaging System." *Journal of Biomedical Optics* 16.8 (2011): 086015.
- Gioux, Sylvain, Amaan Mazhar, David J. Cuccia, Anthony J. Durkin, Bruce J. Tromberg, and John V. Frangioni. "Three-dimensional Surface Profile Intensity Correction for Spatially Modulated Imaging." *Journal of Biomedical Optics* 14.3 (2009): 034045.
- Haeghen, Yves V., Jean Marie A. D. Naeyaert, Ignance Lemahieu, and Wilfried Philips. "A Imaging System with Calibrated Color Image Acquisition for Use in Dermatology." *IEEE Transactions on Medical Imaging* 19.7 (2000): 722–30.
- Hill, Bernard, T. Roger, and F. W. Vorhagen. "Comparative Analysis of the Quantization of Color Spaces on the Basis of the CIELAB Color-difference Formula." *ACM Transactions on Graphics* 16.2 (1997): 109–154.
- Ikeda, Hiroaki, W. Dai, and Y. Higaki. "A Study on Colorimetric Errors Caused by Quantizing Color Information." *IEEE Transactions on Instrumentation and Measurement* 41.6 (1992): 845–849.
- Kim, Soo C., Deok W. Kim, Joon P. Hong, and Dong K. Rah. "A Quantitative Evaluation of Pigmented Skin Lesions Using the L\*a\*b\* Color Coordinates." *Yonsei Med Journal* 41.3 (2000): 333–339.
- Kroll, Stephen S., Mark A. Schusterman, Gregory P. Reece, Michael J. Miller, Gregory R. Evans, Geoffrey L. Robb, and Bonnie J. Baldwin. "Timing of Pedicle Thrombosis and Flap Loss After Free-tissue Transfer." *Plastic and Reconstructive Surgery* 98.7 (1996): 1230–1233.
- León, Katherine, Domingo Mery, Franco Pedreschi, and Jorge León. "Color measurement in L\*a\*b\* units from RGB digital images." *Food Research International* 39.10 (2006): 1084–1091.
- Li-Tsang, Cecilia W., Joy C. Lau, and Sally K. Liu. "Validation of an Objective Scar Pigmentation Measurement by Using a Spectrocolorimeter." *Burns* 29.8 (2003): 779–784.
- Lorenzetti, Fulvio, Juhani Ahovuo, Sinikka Suominen, Asko Salmi, and Sirpa Asko-Seljavaara. "Colour Doppler ultrasound evaluation of haemodynamic changes in free tram flaps and their donor sites." *Scandinavian Journal of Plastic and Reconstructive Surgery and Hand Surgery* 36.4 (2002): 202–206.
- Mahy, Marc, Bertran V. Mellaert, Luc V. Eycken, and André Oosterlinck. "The Influence of Uniform Color Spaces on Color Image-Processing—a Comparative-Study of CIELAB, CIELUV, and ATD." *Journal of Imaging Technology* 17.5 (1991): 232–243.
- Matsui, Aya, Bernard T. Lee, Joshua H. Winer, Rita G. Laurence, and John V. Frangioni. "Quantitative Assessment of Perfusion and Vascular Compromise in Perforator Flaps Using a Near-Infrared Fluorescence-Guided Imaging System." *Plastic and Reconstructive Surgery* 124.2 (2009): 451–460.
- Mazhar, Amaan, Steven Dell, David J. Cuccia, Sylvain Gioux, Anthony J. Durkin, John V. Frangioni, and Bruce J. Tromberg. "Wavelength optimization for rapid chromophore mapping using spatial frequency domain imaging." *Journal of Biomedical Optics* 15.6 (2010): 061716.
- Miyamoto, Kukizo, Hirotsugu Takiwaki, Greg G. Hillebrand, and Seiji Arase. "Development of a digital imaging system for objective measurement of hyperpigmented spots on the face." *Skin Research and Technology* 8.4 (2002): 227–235.
- Pharaon, Michael R., Thomas Scholz, Scott Bogdanoff, David Cuccia, Anthony J. Durkin, David B. Hoyt, and Gregory R. Evans. "Early Detection of Complete Vascular Occlusion in a Pedicle Flap Model Using Quantitation Spectral Imaging." *Plastic and Reconstructive Surgery* 126.6 (2010): 1924–1935.

- Pohlenz, Philipp, Marco Blessmann, Felix Blake, Lei Li, Rainer Schmelzle, and Max Heiland. "Outcome and complications of 540 microvascular free flaps: the Hamburg experience." *Clinical Oral Investigations* 11.1 (2007): 89–92.
- Ponticorvo, Adrien, Eren Taydas, Amaan Mazhar, Thomas Scholz, Hak-Su Kim, Jonathan Rimler, Gregory R. Evans, David J. Cuccia, and Anthony J. Durkin. "Quantitative assessment of partial vascular occlusions in a swine pedicle flap model using spatial frequency domain imaging." *Biomed Optics Express* 4.2 (2013): 298–306.
- Rah, Dong K., Soo C. Kim, Kwang H. Lee, Beyoung Y. Park, and Deok W. Kim. "Objective Evaluation of Treatment Effects on Port-Wine Stains Using L\*a\*b\* Color Coordinates." *Plastic and Reconstructive Surgery* 108.4 (2001): 842–847.
- Russell, John A., Michael L. Conforti, Nadine P. Connor, and Gregory K. Hartig. "Cutaneous Tissue Flap Viability following Partial Venous Obstruction." *Plastic and Reconstructive Surgery* 117.7 (2006): 2259–266.
- Smit, Jeroen M., Paul M. Werker, Anders G. Liss, Morteza Enajat, Geertruida H. de Bock, Thorir Audolfsson, and Rafael Acosta. "Introduction of the implantable Doppler system did not lead to an increased salvage rate of compromised flaps: a multivariate analysis." *Plastic and Reconstructive Surgery* 125.6 (2010): 1710–1717.
- Steele, Matthew H. "Three-Year Experience Using Near Infrared Spectroscopy Tissue Oximetry Monitoring of Free Tissue Transfers." *Annals of Plastic Surgery* 66.5 (2011): 540–545.
- Stokes, Mike, Mark D. Fairchild, and Roy S. Berns. "Precision Requirements for Digital Color Reproduction." *ACM Transactions on Graphics* 11.4 (1992): 406–422.
- Thorniley, Maureen S., Stephen Sinclair, N. J. Barnett, C. B. Shurey, and C. J. Green. "The use of near-infrared spectroscopy for assessing flap viability during reconstructive surgery." *British Journal of Plastic Surgery* 51.3 (1998): 218–226.
- Vakharia, Kalpesh T., Douglas Henstrom, Robin Lindsay, Mary B. Cunnane, Mack Cheney, and Tessa Hadlock. "Color Doppler Ultrasound: Effective Monitoring of the Buried Free Flap in Facial Reanimation." *Otolaryngology—Head and Neck Surgery* 146.3 (2012): 372–376.
- Whitaker, Iain S., George F. Pratt, Warren M. Rozen, Scott A. Cairns, Matthew D. Barrett, Leong Y. Hiew, Mark A. Cooper, and David J. Leaper. "Near Infrared Spectroscopy for Monitoring Flap Viability Following Breast Reconstruction." *Journal of Reconstructive Microsurgery* 28.3 (2011): 149–154.
- Yafi, Amr, Thomas S. Vetter, Thomas Scholz, Sarin Patel, Rolf B. Saager, David J. Cuccia, Gregory R. Evans, and Anthony J. Durkin. "Postoperative Quantitative Assessment of Reconstructive Tissue Status in a Cutaneous Flap Model Using Spatial Frequency Domain Imaging." *Plastic and Reconstructive Surgery* 127.1 (2011): 117–130.

